PRINT ISSN 1119-8362
Electronic ISSN 1119-8362

Full-text Available Online at
https://www.ajol.info/index.php/jasem
https://www.bioline.org.br/ja

J. Appl. Sci. Environ. Manage.
Vol. 26 (3) 487-494 March 2022

Seismic Attribute Analysis for Prospect Delineation in 'TMB' Field, Niger Delta Basin

***ALLO, OJ; BAKO, ME; ESAN, D**

Department of Geosciences, Faculty of Science, University of Lagos, Lagos, Nigeria.
Corresponding Author **Email: allobioje@gmail.com*

ABSTRACT: The 'TMB' Field was evaluated to detect hydrocarbon prospects for the purpose of increasing production volume using seismic attribute analyses. A total of eight sand tops were correlated across the Wells and faults orientation with significant displacement were picked across the field. Three horizons (Res. E, Res. H and Res. J) were used to generate the time maps which were converted to depths by a polynomial function from Time-Depth relationship. Two of the faults are major syn-tectonic growth faults that divides the field into three Fault Blocks (FB1, FB2 and FB3). Seismic attributes (Average Energy, Root Mean Square (RMS), Sweetness and Relative Acoustic Impedance (RAI)) amplitudes were examined to identify hydrocarbon prospect in the reservoirs. An area of interest (prospect) in one of the Fault Blocks (FB3) revealed attribute amplitude responses that suggest the presence of hydrocarbon was identified. The extracted attribute from Average energy, RMS and Sweetness attributes showed high amplitudes similar to attributes obtained from areas around Well log locations (proven area). Normal curves from attribute's histogram distributions support hydrocarbon presence in FB3. The observed prospects are vertically stacked with fault-dependent anticlinal closures that serves as trap within the FB3 fault block.

DOI: **https://dx.doi.org/10.4314/jasem.v26i3.17**

Impact factor: **http://sjifactor.com/passport.php?id=21082**

Google Analytics: https://www.ajol.info/stats/bdf07303d34706088ffffbc8a92c9c1491b12470

Dates: Received: 10 January 2022; Revised: 22 February 2022; Accepted: 15 March 2022

Keywords: Seismic attribute, Faults, Reservoir, Hydrocarbon, Prospect.

In most countries that are endowed naturally with prolific sedimentary basins with large accumulations of hydrocarbons, the oil and gas industry is the primary source of revenue. There have been extensive works done in locating and extracting these hydrocarbons where they are found. In fact, the search for oil and gas, and enhancing recoveries from reservoirs are two of the most important tasks in the petroleum industry. Although the first task requires sedimentological studies of basins and prospect evaluation, the second task requires reservoir description, especially of lithological heterogeneities within a reservoir (Kabaka, 2018; Aminu and Olorunniwo, 2014). Detailed mapping of geological features that are responsible for the formation of hydrocarbon reservoirs has always remain the primary objective of seismic exploration and interpretation (Opara and Osaki, 2018). The ease at which discoveries have been made following the conventional methods have drastically decreased over time. Due to the difficulty in establishing new fields, there has been need to re-visit already discovered fields for chances of detecting by-passing hydrocarbons in these old fields. Therefore, it became imperative for oil and gas explorers to consider new ways of analyzing 3D seismic data so as to further understand the dynamics and behavior of reservoirs in the subsurface. One of these methods is using seismic attributes. Seismic attributes have been used for reservoir characterization, especially since the advent of 3D seismic data. Different studies have shown that seismic attributes are important predictors of reservoir geometries either qualitatively or quantitatively (Hossain, 2019). Also, Sahoo *et al*. (2019) applied seismic attribute analysis and depositional elements to provide a regional reconnaissance interpretation of source, reservoir and seal rock distribution for exploration screening purposes. Ologe *et al*. (2014) worked on the reservoir evaluation of a field in southwestern offshore Niger Delta with the view of identifying the lithological units and quantify the hydrocarbons within the reservoir using petrophysical analysis and inferences. Hydrocarbon prospects in this area were also assessed using seismic attributes. It was

Corresponding Author **Email: allobioje@gmail.com*

observed that the field is characterized by a rollover anticline, with a closed trapping mechanism as well as fault/dip trapping mechanism and the reservoir units are porous with substantial hydrocarbon that were well trapped. Seismic attributes were also used by Opara and Osaki (2018) to enhance reservoir characterization by resolving serious interpretational challenges associated with sub-seismic faults and subtle stratigraphic features. Moreover, Okeke *et al*. (2018) re-evaluated the hydrocarbon prospects in a Niger Delta Field so as to identify unharnessed hydrocarbon prospects, while Hossain (2019) discussed seismic attribute analyses and their usefulness in seismic geomorphology study of the Moragot field, Gulf of Thailand. Attributes from seismic data were used to analyze high amplitude anomaly for potential presence of hydrocarbon in Edi field, Niger Delta (Etuk *et al*., 2020). Although the 'TMB' field has produced reasonable quantity of hydrocarbons in the past within the proven area of the fault block, upon re-processing and quality checking of the seismic data, it is observed that there may be hydrocarbon accumulations that were by-pass or not detected within the field. This has motivated the application of various seismic attributes to investigate this observation in order to identify new areas with probable hydrocarbons presence in the field. In this study, four attributes; RMS amplitude, Average Energy, Sweetness and Relative Acoustic Impedance attributes were used to identify new prospect within the Agbada formation of the "TMB" field, Niger Delta.

MATERIALS AND METHODS

Data Gathering: The dataset used in this study includes 3D post-stack seismic volume in SEG-Y format and it is zero-phased. The in-lines range from 5800 to 6200, cross-lines is from 1480 to 1700 and 400 m by 200 m total coverage with line spacing of 2.51km. Six wells with composite suite of Logs were also provided. The distribution of the Wells within the seismic volume in the study area is shown in the base map (Fig. 1).

Data Loading: Well data were loaded into the software and were subsequently quality-checked. It was observed that almost all logs required for this study were available in each well for loading. However, TMB-01 and TMB-02 lacked both neutron and density logs while Wells TMB-01 and TMB-06 do not have sonic logs as shown in Table 1. Well tops were not provided. All Wells had checkshots which were loaded according to the Wells. TMB-03 and TMB-06 are deviated Wells, they were loaded using the provided Measured Depth (MD), Deviation path and Azimuth data. The seismic volume was also loaded using the seismic coordinate information. While quality-checking the data, it was observed that the seismic character had strong reflections that were continuous across the field. However, in the deeper parts of the seismic volume, the seismic signatures became weak, chaotic and the strong reflections became discontinuous. The seismic is albeit of good quality in general.

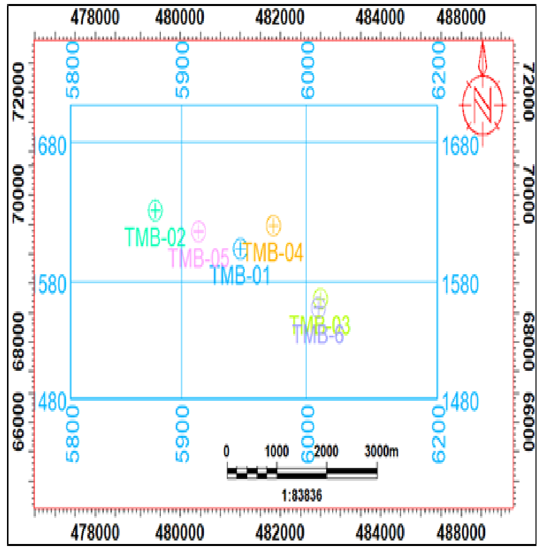

Fig 1: Base Map showing seismic coverage and location of wells, the wells are positioned at their bases

Table 1 Wells and Logs inventory

WELL LOGS	WELLS					
	TMB-01	TMB-02	TMB-03	TMB-04	TMB-05	TMB-06
CALIPER	✓	✗	✓	✓	✓	✓
GAMMA RAY (GR)	✓	✓	✓	✓	✓	✓
SELF-POTENTIAL (SP)	✓	✓	✓	✓	✓	✓
RESISTIVITY, DEEP (LLD)	✓	✓	✓	✓	✓	✓
NEUTRON (NPHI)	✗	✗	✓	✓	✓	✓
DENSITY (RHOB)	✗	✗	✓	✓	✓	✓
SONIC (DT)	✗	✓	✓	✓	✓	✗
EFFECTIVE POROSITY (PHIE)	✓	✗	✓	✓	✓	✓
WELL TOPS	✗	✗	✗	✗	✗	✗
CHECKSHOT	✓	✓	✓	✓	✓	✓

✓ Present ✗ Absent

Data Processing: Well log correlation: The vertical four Wells (TMB-02, TMB-05, TMB-01, TMB-04) were correlated across strike-line. To enable better well correlation, the Wells were referenced at an equal depth value of 2600m SSTVD. The gamma ray log (GR) as well as the resistivity log signatures were used to identify the lithology and hydrocarbon presence respectively.

Seismic to well tie: Seismic to well tie was performed in order to correlate the interpretation done on the logs with seismic observations using checkshot data from TMB-04 as well as its sonic and density logs. The sonic and density logs were convolved by a 30 Hz zero-phase Ricker wavelet to produce the acoustic impedance log from which reflection coefficient (RC) stick was extracted to produce a synthetic seismogram shown in Fig 2. A 15ms bulk shift was applied, which produced 0.762 correlation coefficient, indicating a good character tie. The tie between Well TMB-04, seismic volume and synthetic seismic is shown in Fig. 2.

Fault interpretation: Faults which indicate areas of discontinuity of events, relative termination of reflections and displacement of such reflections were picked along the dip lines. Two of the faults were the major syn-depositional growth faults that divide the field into three fault blocks.

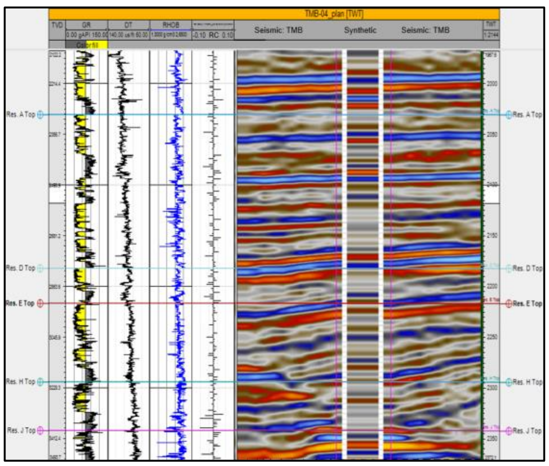

Fig 2: Seismic to well tie from Well TMB-04 showing the synthetic seismogram.

Horizon mapping and Time/Depth map generation: The reservoir tops of interest were identified on the well-logs and consequently mapped across the seismic volume by posting the reservoir tops from the logs to the seismic sections in the time domain. Time maps for the reservoirs were generated by processing the mapped horizons and using a convergent interpolation algorithm. The time structural maps were depth-converted by a second-order degree polynomial Time–Depth relationship generated by the least square method (Fig. 3).

Seismic amplitudes analysis from different reservoir areas: Amplitude extractions were carried out from the proven, brine saturated, as well as the prospective areas of the reservoirs. A portion of the RMS attribute amplitudes that represents the proven, prospect and brine saturated areas were cropped using polygons. The amplitudes from these polygons were then converted to histograms and normal distribution curves were generated from these histograms. These normal curves represent the amplitude distribution plots from each area. However, emphasis was on delineating areas that has not been drilled so as to investigate for opportunities in by-passed prospect.

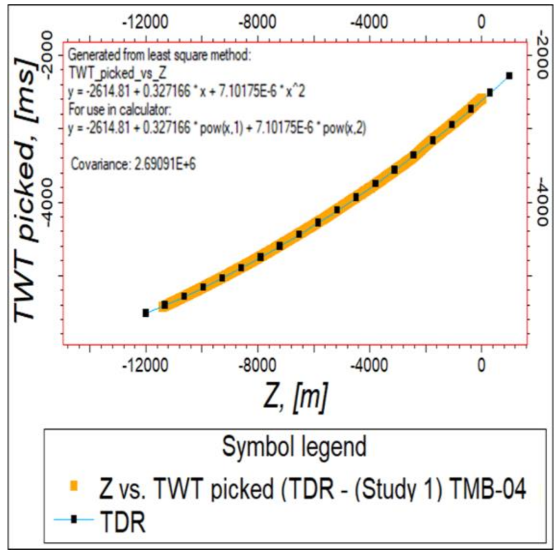

Fig 3: Time-Depth Relationship from TMB-04 used for depth conversion.

Location and Geology of The Study Area: The 'TMB' Field is located at the central part of the coaster swamp depobelt of the Niger Delta basin. It is situated within latitude $4°N$ and $6°N$, while it is within longitude $6°E$ and $7°E$, covering an area of 55 km^2 as shown in Fig. 4. The in-lines and cross-lines are in the ranges of 5800 to 6200 and 1480 to 1700 respectively, while a spacing of 25m between the lines.

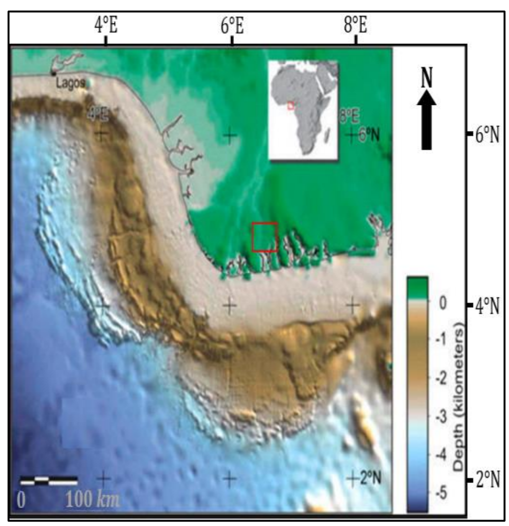

Fig 4: Location of 'TMB' Field (red rectangle) in the Niger Delta Basin (Modified after Emakporue and Ofuyah, 2019).

Niger Delta Structural Style: Growth faulting dominates the structural style, which is interpreted to be triggered by the movement of deep-seated, over pressured, ductile marine shale and aided by slope instability (Obaje, 2009). Faults flatten with depth into a detachment plane near the top of the over pressured, marine shale sequence. Hanging wall rollover anticlines developed as a result of listric-fault geometry and differential loading of deltaic sediments above ductile shales (Doust and Omatsola, 1990). There is the occurrence of shale diapirs in the Delta and these diapirs are of three types; the first type is the zone behind major faults, while the second type are those shale that bulges in front of the growth faults (Fig. 5). The third types are those that extended in a sea ward direction as a result of differential loading on the plastic marine shale (Doust and Omatsola, 1990; Emakporue and Ofuyah, 2019).

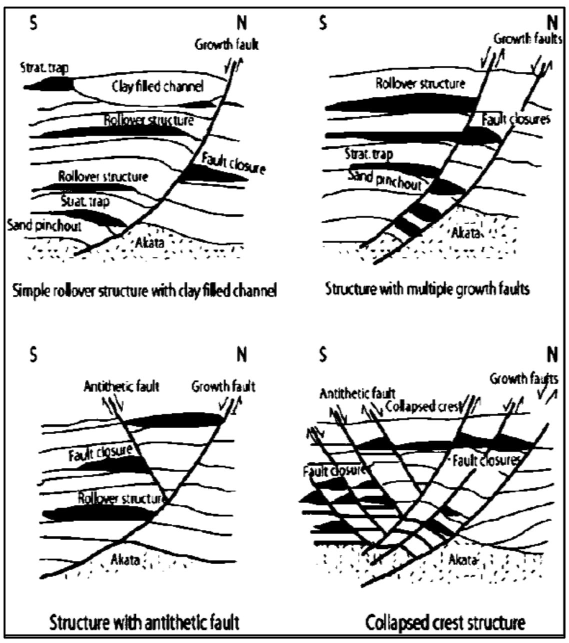

Fig 5: Tec*tonic* structures and associated traps (Doust and Omatsola, 1990).

Stratigraphic Fill of the Niger Delta: The Formations in the Niger Delta are made up of three stratigraphic columns (Aminu and Olorunniwo, 2014). An upper delta top lithofacies known as the Benin formation consist of marine continental sand and gravel. This fresh water bearing continental clastic grades down into and overlies uncomfortably the delta front lithofacies called the Agbada formation which is a paralic unit of brackish water origin comprising mostly shoreline and channel deposit with minor shale in the upper part and the alternative of sand and shale in equal proportion in the lower part (Doust and Omatsola, 1990; Evamy *et al*., 1978; Etuk *et al*., 2020).

The pro-delta marine shales belonging to the Akata formation occur deeper in the sequence thus underlining the Agbada formation (Tuttle *et al*., 1999). This formation is associated with sandstone units only in generally lowstand turbidite fans deposited in a deep marine setting. Characteristically, the marine shales are under-compacted and over-pressured, thus often undergoing diapirism.

RESULTS AND DISCUSSION

Well correlation: The Well correlation panel in Figure 6 revealed sandstone reservoir with similar Gamma Ray (GR) signatures across the Wells. Eight horizons were correlated across the field, three reservoirs Res. E, Res. H and Res. J are of interest because of the presence of hydrocarbon shown by its high resistivity signatures. These reservoirs are all within the time range of -2000 ms to -2550 ms on seismic, where correlation of the reservoirs with significant lateral continuity is revealed as indicated in Figs. 6 and 7.

Fault trend interpretation: The faults were observed to be dipping in the West–East direction (Fig. 7). Three fault blocks were identified based on the displacements observed at the fault planes. Two of the faults are the main syn-depositional growth faults, induced by gravity tectonism and have mostly offset different parts of the Agbada formation. However, it flattens out near the top of the Akata formation (Fig. 7) as supported by (Doust and Omatsola, 1990; Nwajide, 2013). The drilled Wells are concentrated in Fault block 2.

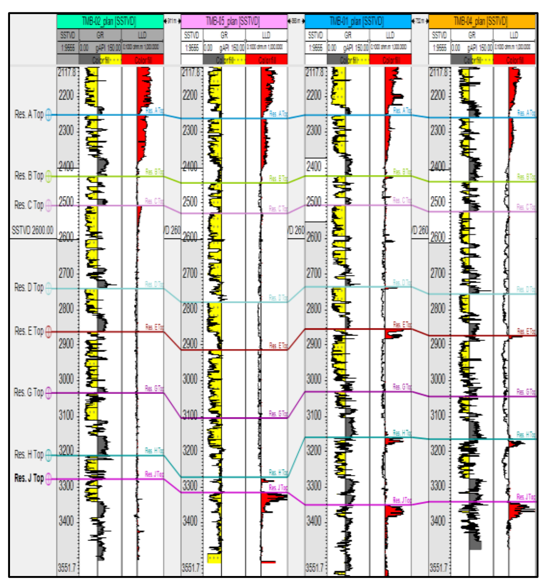

Fig 6: Well log correlation across four wells along the strike line in the study area

The generated surface depth map of Reservoir E (Res. E) is shown in Fig. 8a. This map illustrates the fault orientation and also the direction of cross–sections A–B and X–Y. Figs. 8 (b and c) are vertical cross–sections across the fault blocks that has not been drilled. It revealed multiple level stacking pattern of sands and shales seismic events. The trapping style is indicative of fault–dependent closures facilitated by the growth faults (Figs. 8a and 8b) as earlier discussed in Doust and Omatsola (1990), and Nwajide (2013).

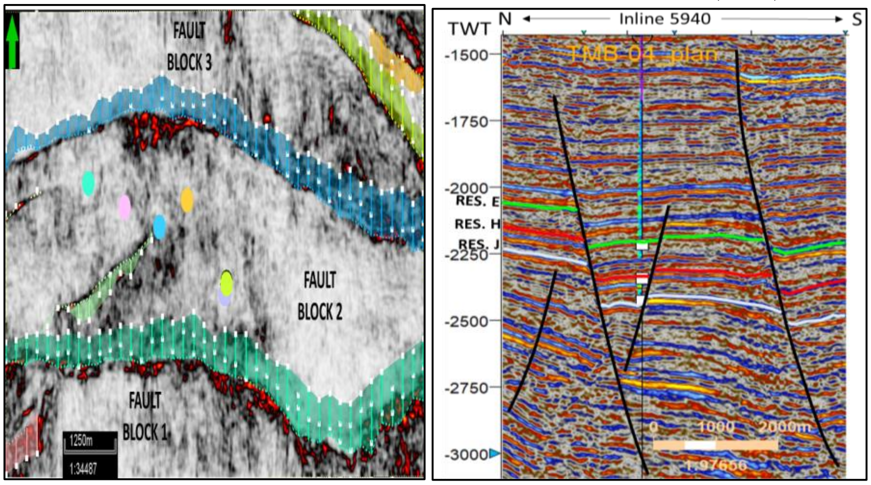

Fig 7: Time slice at -2240ms showing three main fault blocks with Well locations in Fault block 2, and seismic section on the right-hand side indicating fault planes with the reservoir horizons.

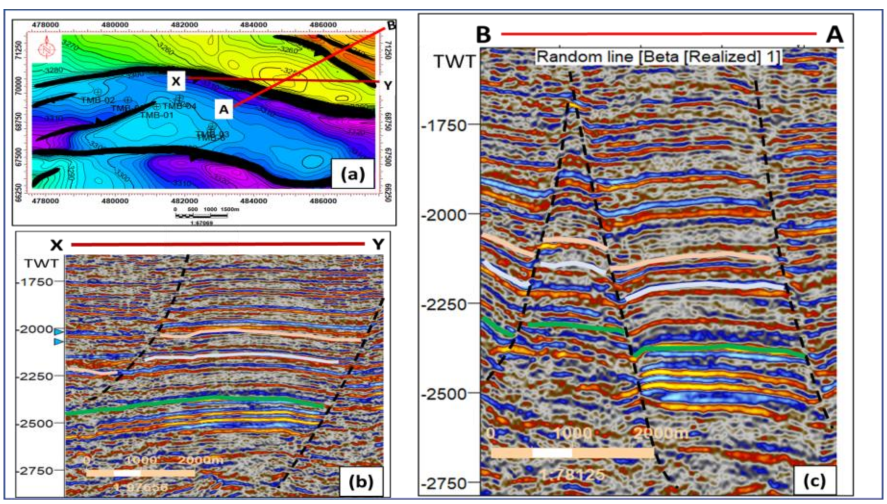

Fig 8: (a) Surface depth map of Reservoir E showing fault trends and lines of vertical cross–sections. (b) Vertical cross–sections along line X–Y and (c) Vertical cross–section along line A–B showing stacking pattern of prospects trapped by fault-dependent closures

Prospect Detection from Seismic Attributes: Extracted Average Energy, RMS and Sweetness attributes from surface maps of the three reservoirs (Res. E, Res. H and Res. J) revealed high amplitude signature at the identified prospect situated in Fault Block 3, North–East area of the field. This prospect is highlighted by the 'red dash oval' shown in Figs. 9 (a, b and c). The maps reveal high amplitudes zone that are similar to the amplitudes around the proven area (Fault block 2) where the Wells are located (red ovals). Similarly, the contour lines in the prospect area illustrate that the amplitudes conform to fault structure which serve as trap that prevents hydrocarbon migration. The area represented by the 'red square' is brine saturated due to the consistent low amplitude response observed in the area from all the attributes amplitude. Other areas that reveal high amplitudes do not conform to fault structure. It thereby reduces the chance of being a hydrocarbon reservoir. However, Relative Acoustic Impedance (RAI), does not show significantly high amplitudes in the prospect area (Fig. 9d). The RAI is based on impedance contrast between reservoirs and its encompassing lithologies. Although, RAI amplitudes from the proven areas are relatively high, the relatively low amplitude from the prospect area is due to low impedance contrast between the hydrocarbon reservoir and the surrounding shale lithology. This implies that the presence of hydrocarbon which has lower density/velocity values compared to water (brine) will result to reduction in its impedance. This will in turn reduce the contrast between the reservoir and the surrounding shale lithology, and eventually reduced seismic amplitude signal as described in Emakporue and Ofuyah (2019), Simm and Bacon (2014), and Mavko *et al*. (2003). Similar scenarios of attribute responses are observed in the other two reservoirs (Res. H and Res. J).

Seismic attribute amplitude distributions: The cropped areas, bounded by polygon which are the proven, prospect and brine saturation are shown in Fig. 10.

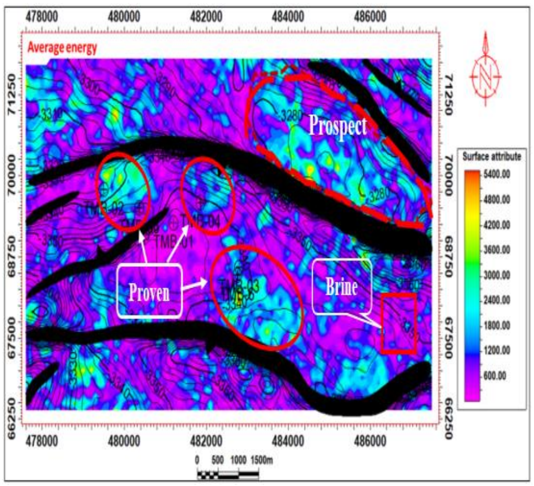

Fig 9a: Average energy attribute of Reservoir E showing high amplitudes around the Well locations (red ovals) and prospect area (red dash oval). The red square area is a low amplitude area which represent water (brine) saturation.

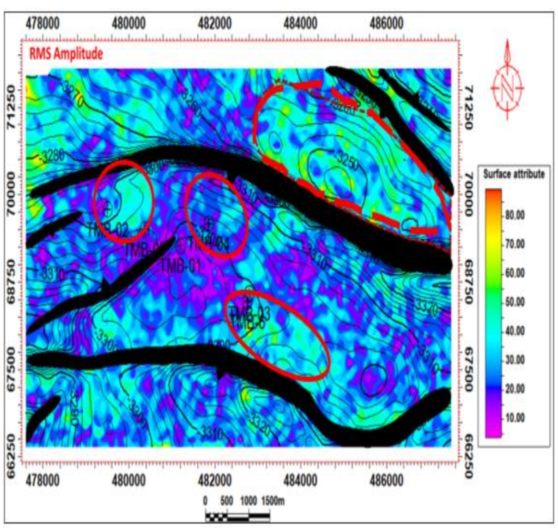

Fig 9b: RMS attribute of Reservoir E showing high amplitudes around the Well locations (red ovals) and prospect area (red dash oval).

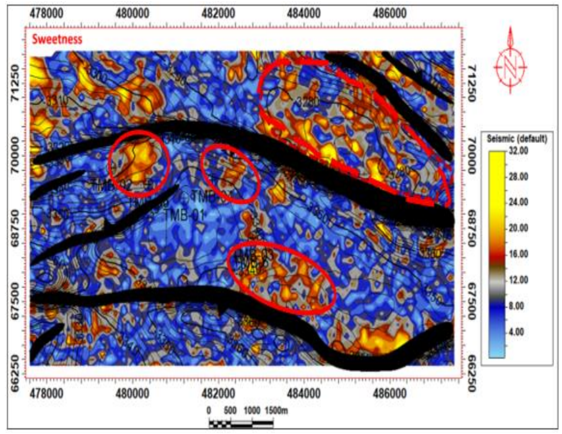

Fig 9c: Sweetness attribute of Reservoir E showing high amplitudes around the Well locations (red ovals) and prospect area (red dash oval).

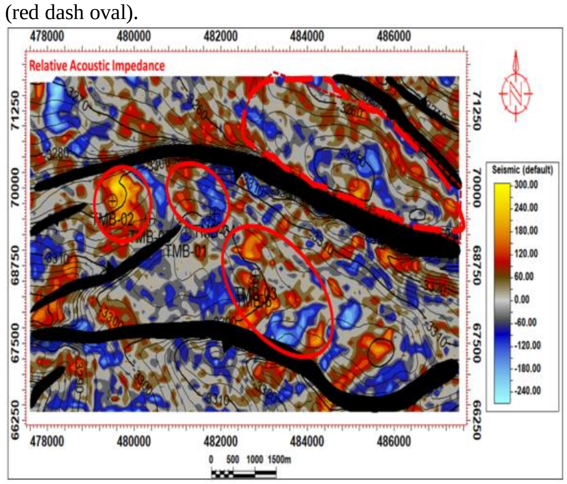

Fig 9d: Relative Acoustic Impedance (RAI) attribute of Reservoir E showing high amplitudes around the Well locations (red ovals) and low amplitudes prospect area (red dash oval).

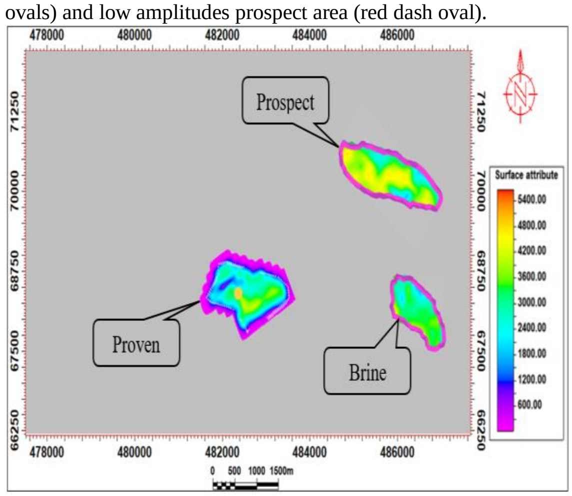

Fig 10: Cropped locations bounded by polygon around the proven, prospect and brine saturation areas from the surface attribute amplitude map of Res. E.

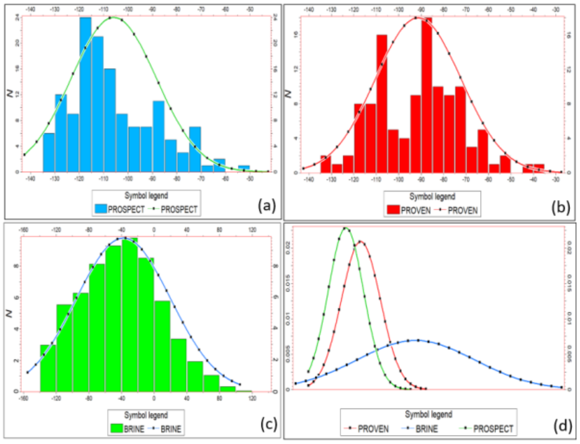

Fig 11: Attribute amplitude histogram plots overlaid with normal distribution curve at the (a) proven area (b) prospect area and (c) brine saturated area. (d) shows only the overlay of normal distribution curves from these areas.

Histogram distribution (amplitudes versus frequency of occurrence, N) of the surface attribute amplitude from Res. E with the overlay of normal distribution curve of these areas are shown in Figs. 11 (a, b and c). The normal plot trends show good agreement between the prospect and proven areas of the Res. E, suggesting occurrence of similar fluid (hydrocarbon) in both Fault Blocks 2 (FB2) and 3 (FB3) as shown in (Figs. 11d).

Conclusions: In this study, reservoirs were evaluated for prospect delineation by examining amplitudes from seismic attributes. Relationships between well log interpretations and seismic reflections revealed that three reservoirs separated into fault blocks by regional faults influenced the architecture and geometry of the reservoirs. Also, similar amplitude anomalies were observed in the prospect (Fault Block 3) and the proven areas. The prospect areas conformed to a four-way anticlinal closure exhibiting stacking pattern of multiple sand levels with likely hydrocarbon saturation.

Acknowledgements: The authors wish to acknowledge the Earth Signature Research Group (ESReG), Department of Geosciences, University of Lagos and Department of Petroleum resources for making this study come to reality.

REFERENCES

Aminu, MB; Olorunniwo, MA (2014). Multi-attributes prediction of lithology and porosity from seismic data over Tomboy Field, Niger Delta. *J. of Min. and Geol*. 45(1): 13–20.

Doust, H; Omatsola, E (1990). Niger Delta. In: Edward, JD; Santogrossi, PA (ed). Divergent and Passive Basins. *The Ameri. Assoc. of Pet. Geol.* 239–248.

Emakporue, G; Ofuyah, W (2019). A spectral method of lithofacies differentiation within a hydrocarbon reservoir unit using seismic and well data from Tomboy Field Niger Delta. *J. of Environ and Earth Sci*. 9(3): 146–169.

Etuk, NO; Aka, M; Agbasi, OE; Ibuot, J (2020). Evaluation of seismic attributes for reservoircharacterization over Edi field, Niger delta, Nigeria using 3d seismic data. *International J. of Advan. Geosci*. 8(2): 168–172.

Evamy, B; Haremboure, J; Kamerling, P; Knaap, W; Molloy, F; Rowlands, P; (1978). Hydrocarbon habitat of Tertiary Niger Delta. *Ameri. Assoc. of Pet. Geol. Bull*. 62: 277-298

Hossain, S (2019). Application of seismic attribute analysis in fluvial seismic geomorphology. Journal of Petroleum Exploration and Production Technology. https://doi.org/10.1007/s13202-019-00809-z.

Kabaca, E (2018). Seismic stratigraphic analysis using multiple attributes - An application to the F3 block, offshore Netherland. M.Sc. Dissertation, The University of Alabama.

Koson, S; Chenrai, P; Choowong, M (2014). Seismic attributes and seismic geomorphology. *Bull. Earth Sci. Thailand*. 6(1): 1–9.

Mavko, G; Murkeji, T; Dvorkin, J (2003). The Rock Physics Handbook. Cambridge: Cambridge University Press, UK.

Nwajide, C (2013). Geology of Nigeria's sedimentary basins. CSS press, Lagos.

Obaje, NG (2009). Geology and mineral resources of Nigeria, Berlin, Springer. https://doi.org/10.1007/978-3-540-92685-6

Okeke, HC; Okoro, A; Ezediegwu, PC; Chinwuko, AI; Onuigbo, EN; Omeokachie, A (2018). Evaluation of Hydrocarbon Prospect of Tomboy C-field Offshore Niger Delta, Nigeria. *J. of Basic Phys. Res*. 8(2): 65–78.

Ologe, O; Bakole, S; Oke, S (2014). Hydrocarbon Prospecting Over 'Ok' field, Niger Delta UsingPetrophysical and Seismic Attributes Analysis. *Nig. J. of Technology*. 33(3): 40–408.

Opara, AI; Osaki, LJ (2018). 3–D Seismic attribute analysis for enhanced prospect definition of "Opu Field", Coastal Swamp Depobelt Niger Delta. Nigeria. *J. of Appl. Sci*. 18(2): 86-102.

Perez de Pottella, VI (2012). 3–D Seismic interpretation, seismic attribute analysis and well log interpretation of an area between Ellis and Rooks Counties, Kansas. M.Sc. Dissertation, Fort Hays State University, Kansas.

Sahoo, TR; Hill, M; Browne, GH (2014). Seismic attribute analysis and depositional elements in the Canterbury Basin. Geotechnical Petroleum Forum, Wellington, New Zealand.

Schlumberger (2007). Interpreter’s Guide to Seismic Attributes Manual. Schlumberger.

Simm, R; Bacon, M (2014). Seismic Amplitude. An interpreter’s handbook. Cambridge University Press, UK.

Taner, MT (1997). Seismic trace attributes and their projected use in prediction of rocks propertiesand seismic facies. Rock Solid Images, Switzerland.

Tuttle, M; Charpentier, R; Brownfield, M (1999). The Niger Delta Petroleum System: Niger Delta Province, Nigeria, Cameroon, and Equatorial Guinea, Africa. USGS, Open File Report 9950-H.